Journal Pre-proof

Plio-Pleistocene rear-arc volcanism in the Southern Volcanic Zone: Eruptive styles of the Varvarco Volcanic Field

S.B. Iannelli, V.D. Litvak, A. Folguera

PII: S0895-9811(23)00464-9

DOI: https://doi.org/10.1016/j.jsames.2023.104652

Reference: SAMES 104652

To appear in: *Journal of South American Earth Sciences*

Received Date: 31 July 2023

Revised Date: 3 October 2023

Accepted Date: 11 October 2023

Plio-Pleistocene rear-arc volcanism in the Southern Volcanic Zone: Eruptive styles of the Varvarco Volcanic Field

Iannelli, S. B.[1,2], Litvak, V. D.[1,2], Folguera, A.[1,2]

[1] Departamento de Ciencias Geológicas, Universidad de Buenos Aires, Buenos Aires, Argentina.

[2] Instituto de Estudios Andinos 'Don Pablo Groeber', CONICET- Universidad de Buenos Aires, Buenos Aires, Argentina.

Corresponding Author: Sofía B. Iannelli, sofia.iannelli@hotmail.com.ar, sofiab.iannelli@gmail.com

Abstract

The Varvarco Volcanic Field (VVF) is located in the southern part of the Las Loicas Trough, as part of the Late Pliocene-Early Pleistocene rear-arc volcanic belt in the Transitional Southern Volcanic Zone (34.5-37°S). Its volcanic products show an elliptical distribution, elongated parallel to NW-SE main structures that regionally controlled the Las Loicas Trough. A detailed field and petrographic study was carried out to identify main lithofacies and establish its eruptive styles.

The VVF magmatic evolution is initially characterized by a voluminous explosive stage represented in the area by dense and dilute pyroclastic density currents (PDC) deposits (massive lapilli tuffs, cross-stratified lapilli tuffs and diffuse-stratified tuffs). Afterwards, it evolved into an effusive stage represented by basaltic lava flows (coherent basalts), associated with Hawaiian to Strombolian eruptive style, which constitutes most of the VVF volume. The final stage of the VVF history was linked to a stratovolcano-type activity where both effusive (coherent basalts and andesites, and rhyolitic coulees) and explosive lithofacies (such as massive lithic breccias and massive lapilli tuffs) are described. Within this stage, the uppermost effusive levels were intruded by dacitic and rhyolitic domes and basaltic dykes. Available ages allow to conclude that the VVF emplacement was developed during Plio-Pleistocene times, linked to the re-steepening of the Nazca plate, after the Late Miocene Payenia shallow subduction regime.

Keywords: Andean rear-arc magmatism, Transitional Southern Volcanic Zone, Pliocene-Pleistocene, Volcanic lithofacies description.

1. Introduction

The Southern Volcanic Zone (SVZ) in the Southern Central Andes includes a wide variety of Cenozoic volcanoes with different eruptive histories and an extensive areal distribution from the volcanic arc-front to the back-arc zone (e.g., Hickey et al., 1984; Hildreth and Moorbath, 1988; Stern, 2004; Hickey-Vargas et al., 2016). The emplacement and evolution of these volcanic fields have been controlled by several factors such as slab geometry, convergence rate and direction, the involvement of oceanic sediments in the magmatic source, the presence of slab fluids, the interaction with the continental crust, and the prevailing tectonic setting (e.g., Stern, 2004; Cembrano and Lara, 2009). In turn, the Southern Volcanic Zone has been divided into four areas: the Northern, Transitional, Central and Southern Southern Volcanic Zones, according to their main magmatic characteristics (see Jacques et al. 2014 and references therein) (Fig.1a). In this work, we focus on the description of the eruptive styles of one of the most outstanding and voluminous rear-arc volcanic centers of the Transitional Southern Volcanic Zone (TSVZ) (34.5-37°S): the Varvarco Volcanic Field (Figs. 1a, b).

The evolution of the Neogene to Quaternary magmatism in the TSVZ has been related to the variable Nazca plate subduction angles that modified the location of the magmatic arc front through time (e.g., Kay et al., 2006; Ramos and Folguera, 2011). Thus, arc-like magmatic evolution during this period was directly associated with the transition from a Late Miocene shallow subduction to the present normal slab subduction setting (e.g., Kay et al., 2006; Soager et al., 2013). The Early to Late Miocene shallower configuration of the Nazca plate provoked the expansion of arc-like magmatism towards the east (Ramos et al., 2014; Litvak et al., 2015). After Pliocene times (~3.5 Ma), the Nazca plate subduction angle increased and an extensional tectonic regime was installed (Pesicek et al., 2012). The steepening of the Nazca plate led to the retraction of arc-like magmatism from east to west, resulting in the establishment of three magmatic belts located in the back-arc, rear-arc, and volcanic arc-front areas, respectively (Fig. 1b).

Late Pliocene times in the TSVZ are characterized by the development of the Basaltic Payenia Province in the back-arc, which comprises a widespread voluminous intraplate-like basaltic magmatism with almost no slab-fluids influence (e.g., Holm et al., 2016; Soager et al., 2013; Germa et al., 2010; Pallares et al., 2016) (Fig. 1b). Magmatism in this belt is distributed among different volcanic fields, which are, from north to south: the Northern Segment, Nevado, Llancanelo, Río Colorado and Auca Mahuida volcanic fields (Fig. 1b). Variable geochemical signatures characterize their volcanic products along strike, and so, different mantle sources have been proposed for each one: the northern ones show an Atlantic MORB-type mantle, while the southern ones point to an EM1 OIB-type mantle source (Gudnason et al., 2012; Soager et al., 2013; Espanon et al., 2016; Holm et al., 2016).

During the steepening of the Nazca plate, arc-like magmatism continued retracting towards the west, developing a Late Pliocene-Early Pleistocene N-S magmatic belt located in a rear-arc position (Muñoz Bravo et al., 1985; Hildreth et al., 1999; Jacques et al., 2013). This area is mainly characterized by extensional structures that control, at its southern part (35º30'-37ºS), the development of Las Loicas Trough (35º-37ºS), hosting stratovolcanoes, dome complexes, and calderas (Folguera et al., 2006) as the Puelche (Hildreth et al., 1999), Calabozos (Hildreth et al., 1984), and the Laguna del Maule volcanic fields (Frey et al., 1984; Hildreth et al., 2010), and southwards, the Domuyo (Galetto et al., 2018; Astort et al., 2019) and Tromen volcanic centers (Folguera et al., 2008; Pallares et al., 2019) (Fig. 1b). Further north (34°-35º30'S), Pliocene to Holocene magmatic activity is characterized by the development of minor monogenetic cones and stratovolcanoes as the Overo, Sosneado and Risco Plateado volcanoes, mostly characterized by basaltic-andesitic to dacitic lava flows and interbedded pyroclastic deposits (Fuentes and Ramos, 2008; Folguera et al., 2009; Sruoga et al., 2016) (Fig. 1b).

Finally, the volcanic arc-front magmatism retracted to its current westernmost position in the late Pleistocene to Holocene times. The arc-front magmatism is represented by a series of stratovolcanoes and monogenetic cones with a basaltic to andesitic composition (Fig. 1) (Dungan et al., 2001; Sellés et al., 2004; Sruoga et al., 2012; Tormey et al., 1995, 1991), and a variable geochemical signature along the Andean margin, expressing mainly variations in crustal thickness and subducted slab geometry (Stern and Skewes, 1995; Hickey-Vargas et al., 2016; Turner, 2017). Besides, arc-front magmatism in the TSVZ is influenced by MORB-type altered oceanic crust and overlying marine sediments (Hildreth and Moorbath, 1988; Sellés et al., 2004; Jacques et al., 2013), characterized by several fracture zones, as the Mocha Fracture Zone (MFZ) at 36ºS.

Within this context, the Varvarco Volcanic Field (VVF) is located in the southern part of the Las Loicas Trough, as part of the Late Pliocene-Early Pleistocene rear-arc volcanic belt. The VVF is an example of voluminous arc-like magmatism located in a distant position form the trench and the coetaneous volcanic arc front. Here, we focus on the lithofacies description and the eruptive mechanisms that controlled this magmatism during its emplacement by Plio-Pleistocene times.

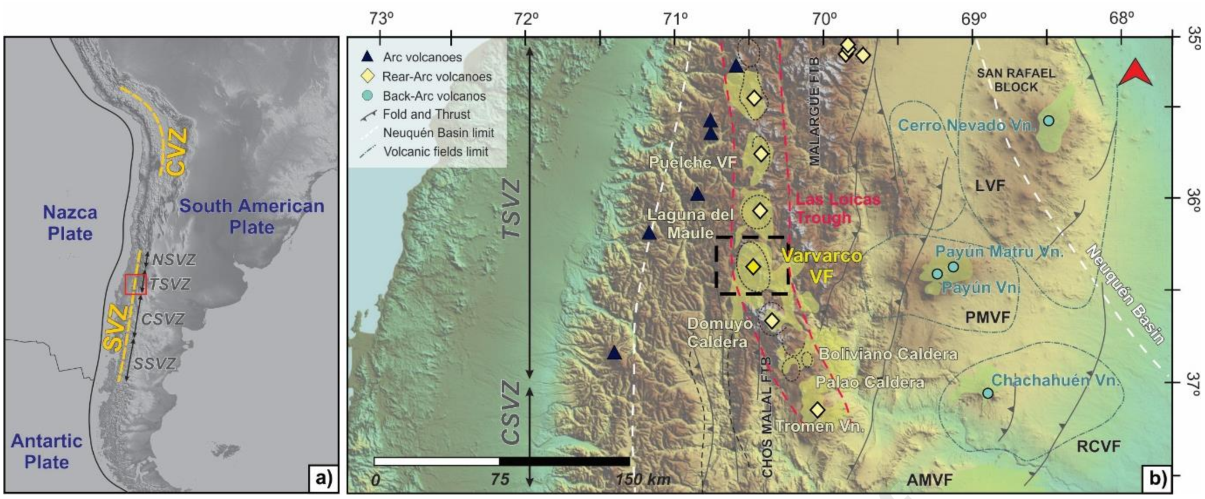

Fig. 1. (a) Location of the studied area in the Transitional Southern Volcanic Zone. (b) Distribution of the Cenozoic magmatism in the three main magmatic belts in the retro arc, rear arc and volcanic arc zones (based on Folguera et al., 2009, Hickey-Vargas et al., 2016, Jacques et al., 2013, Pallares et al., 2016; Søager et al., 2013). Abbreviations: LVF = Llancanelo Volcanic Field, PMVF = Payún Matrú Volcanic Field, RCVF = Río Colorado Volcanic Field; AMVF = Auca Mahuida Volcanic Field.

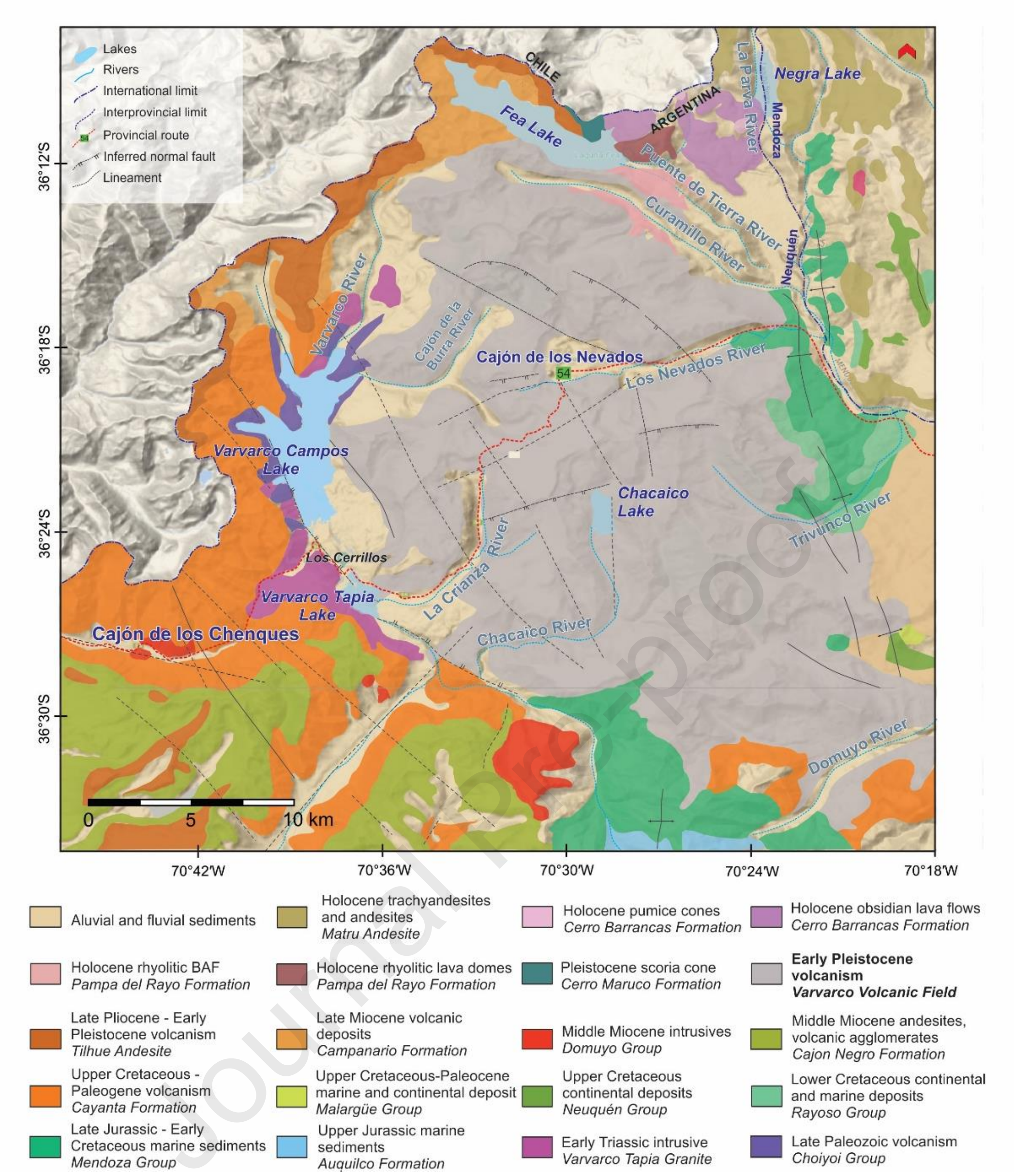

Fig. 2. Main geological units that crop out in the surroundings of the Varvarco Volcanic Field (based on Zanettini, 2001; Narciso et al., 2004; Sruoga et al., 2017).

2. Geological setting of the Varvarco Volcanic Field

The Varvarco Volcanic Field (VVF) is located in the Southern Central Andes, in the TSVZ (34.5-37°S) (e.g., Lopez-Escobar et al., 1995; Stern, 2004). It is emplaced over a heterogeneous basement composed of Late Paleozoic ignimbrites of the Choiyoi Group (e.g., Kleiman and Japas, 2009) that outcrop surrounding the Varvarco Campos Lake (Fig. 2). Early Triassic granitic intrusions were lately emplaced associated with the same magmatic episode and represented in the area by the Varvarco Tapia granites nearby the Varvarco Campos Lake (Zanettini, 2001) (Fig. 2). Jurassic to Cretaceous sedimentary outcrops in the studied area are linked to the development of the Neuquén Basin, which are recognized mainly in the eastern part (Fig. 2) (Tunik et al., 2010; Horton et al., 2016; Tapia et al., 2020). Magmatism dominated the studied area since the Upper Cretaceous and Paleocene times, represented by the explosive and effusive volcanism of the Cayanta Formation (Fig. 2). Later, Middle Miocene calc-alkaline magmatism is associated with the volcanic agglomerates and andesitic rocks of the Cajón Negro Formation that represented a period of eastward magmatic arc expansion (Pesce et al., 1981), and so associated with the Nazca plate shallow subduction period (e.g., Ramos et al., 2014).

Afterwards, in the Late Pliocene to Quaternary times, the re-steepening of the Nazca plate began and in consequence an extensional regime established (Pesicek et al., 2012; Ramos et al., 2014). Within this context, a volcano-tectonic basin, defined as Las Loicas Trough, was developed, which was controlled by N-NE extensional structures (Fig. 1b) (Ramos and Kay, 2006; Folguera et al., 2006). The northern sector of this depocenter is characterized by an eastern N-S normal fault with a west inclination defining a half-graben structure where the prevailing products are andesitic lavas, ignimbrites and ash fall deposits (Hildreth et al., 1999) (Fig. 2). The southern part of this basin shows silicic centers and basaltic-andesitic stratovolcanoes, where the studied VVF is located (e.g., Kay et al., 2006; Pallares et al., 2019) (Fig. 1b).

The VVF magmatism has been initially described as a volcanic caldera considering its elliptic geometry, presence of basal explosive products, large amount of lava flows and domes and its association with other magmatic calderas in the area (Folguera et al., 2006) and was formerly included in variable units such as the Tilhue Andesite and the Coyocho Formation (Zanettini, 2001; Kay et al., 2006; Pallares et al., 2019).

Recent studies have described the VVF as formed by voluminous basaltic lava flows associated with pyroclastic deposits in its basal levels and with rhyolitic to andesitic lavas towards the top; while dacitic to rhyolitic intrusives and basaltic dykes affect the middle to upper levels of the sequence (Iannelli et al., 2022). The basal section of the VVF magmatism would be Early Pleistocene regarding a U/Pb zircon age (2.36 Ma) made over a vitreous tuff located in the basal stratigraphic levels (Iannelli et al., 2023).

The youngest units within the studied area are Holocene rhyolitic lava flows and domes (Pampa del Rayo Formation) and obsidian lava flows (Cerro Barrancas Formation), which represents the latest magmatic episodes of the Laguna del Maule Volcanic Field located to the north between the Fea and Negra Lakes (Sruoga et al., 2017) (Fig. 2).

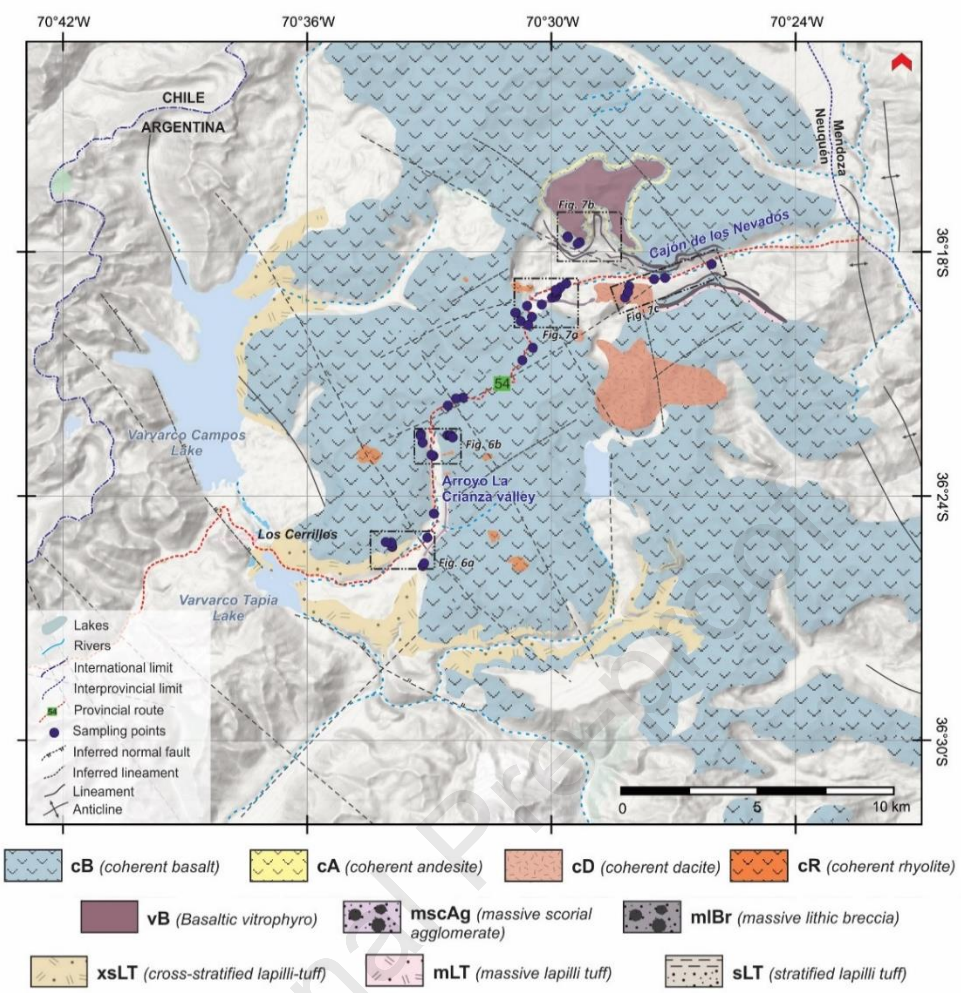

Fig. 3. Detailed map of the Varvarco Volcanic Field showing the main volcanic lithofacies recognized in the area. Blue dots show the samples' location while the black squares indicate the stratigraphic profiles' locations.

3. Methodology

In this work, we present detailed field and petrographic descriptions of the main volcanic lithofacies that characterized the studied VVF magmatism, whose distribution is shown in the map of Figure 3. Five stratigraphic profiles were made along the studied area. Detailed descriptions of the main lithofacies, their structure and spatial relationships are included. Fifty thin sections were described using a Leica DP750 microscope with the aim of better understanding the compositional and textural variations of the VVF volcanic products. A volcanic lithofacies analysis was made considering the field and petrographic features of each volcanic and volcano-sedimentary level.

To approach the lithological description of the VVF products, McPhie et al. (1993) scheme was firstly considered to define genetic classification of volcanic deposits. Besides, the definition and classification of the variable lithofacies that characterized the VVF (Table 1) has been made following recommendations of Branney and Kokelaar (2002), while pyroclastic rock nomenclature and classification was made according to Schmid (1981). In specific cases, new lithofacies were named for achieving a better characterization of volcanic features and units (Table 1).

4. Results

4.1. Petrography and lithofacies description

The Varvarco Volcanic Field (VVF) is mainly characterized by a basal silicic ignimbritic deposit followed by basaltic porphyritic lava flows, which are interbedded with minor vitreous tuff levels, and intruded by rhyolitic to dacitic intrusives and basaltic dykes (Figs. 4, 5, 6). The studied magmatic sequence covers a semielliptical area of 840 km^2, as shown in the detailed map of Figure 3. The Varvarco Volcanic Field is divided into two main areas: the Cajón de Los Nevados area to the northeast and the Arroyo La Crianza area to the south (Fig. 3).

Following the genetic classification proposed by McPhie et al. (1993), the VVF volcanic sequence includes effusive and explosive deposits. Within the effusive activity, we described both coherent lavas and autoclastic deposits, while the explosive activity is mainly represented by pyroclastic fall and pyroclastic density currents (PDCs) deposits (Branney and Kokelaar, 2002).

Detailed field and petrographic descriptions have been made to constrain the most important lithological differences and to define non-genetic lithofacies to precise the magmatic sequence of the Varvarco Volcanic Field, its eruptive styles and emplacement history. Particularly, fourteen lithofacies have been recognized following McPhie et al. (1993) and Branney and Kokelaar (2002) recommendations.

4.1.1. cB (coherent basalts)

The coherent basalts (cB) lithofacies are the most predominant volcanic lithofacies of the VVF (Figs. 4, 5, 6). They show almost similar macroscopic features, differing solely in the amount of phenocrysts and in the presence of vesicles. However, main differences are seen under the microscope due to variations in the amount and type of the most dominant mafic minerals and variable glass content between the different levels.

The coherent basalts (cB) outcrop as extensive tabular layers (20-50 m thick), sometimes interbedded with autoclastic and pyroclastic deposits (Figs. 4a, 4c, 4d, 5d, 6a). Some cB flow levels of 25 m thick, especially in the basal parts, show well-developed columnar jointing (Figs.

4e, f). They are dark grey rocks with porphyritic texture composed of plagioclase, olivine and mafic phenocrysts immersed in an aphanitic groundmass (60-90%). Locally, the cB show aphanitic textures and vesicles.

Microscopically, the cB are fresh and porphyritic rocks, composed of plagioclase (45-65%), clinopyroxene (20-30%), orthopyroxene (10-20%), olivine (25-10%) and opaque minerals (5-10%) (Figs. 4g, 5c, 6c) although minor aphyric rocks have also been identified. The groundmass (60-95%) varies from intergranular to intersertal and is mainly composed of plagioclase microlites, pyroxenes and opaque minerals. The glass, when is present, is mainly fresh with a light-brown color, although it can also be partially altered to clays. Some of these basaltic levels show a variable percentage of vesicles; when they prevail, we include them in a sub-lithofacies named as vesicular coherent basalts (cBv).

Interpretation: Field and thin-sections descriptions indicate that the cB rocks correspond to basaltic lava flows. The well-development columnar jointing described in the basal levels would indicate long time intervals of solidification (Cas and Wright, 1988). The vesicular coherent basalts (cBv) lava flows, particularly located above the cB lithofacies, might represent the uppermost level within a unique subaerial lava pulse.

4.1.2. cA (coherent andesites)

The coherent andesites (cA) lithofacies is mainly described in the Cajón de Los Nevados valley, being less abundant than the coherent basalts (cB). The cA outcrops as subhorizontal light grey levels 10 to 15 m thick (Figs. 6d, e). They are porphyritic volcanic rocks composed of plagioclase (85%) and mafic minerals (15%) in a light grey groundmass (60%).

Microscopically, they show a porphyritic to glomeroporphyritic texture composed of plagioclase (70%), amphibole (15%), orthopyroxene (10%), and clinopyroxene (5%) phenocrysts. Plagioclase is fresh with simple twinning and compositional zoning (Fig. 6f). The amphibole phenocrysts are partially fresh and show brownish pleochroism and resorption rims (0.3-1.5 mm length); orthopyroxenes are subhedral (0.3-0.7 mm) and lightly altered to orange clays, while clinopyroxenes show a maximum length of 0.3-1 mm. The groundmass (65%) consists of small microlites of plagioclase, pyroxene and opaque minerals, and variable amount of glass, showing an intergranular to hyalopilitic texture.

Interpretation: Similarly to the cB, the cA lithofacies is interpreted as subaerial lava flows, in this case, of andesitic composition.

4.1.3. cD (coherent dacite)

The coherent dacite (cD) lithofacies is mainly identified in the Cajón de Los Nevados area (Fig. 3). They comprise globose-shaped bodies of 5 km in diameter, which intrude the coherent basalts (cB) and massive lithic breccias (mlBr) lithofacies (Fig. 5a). The outcrops are light pink in color and show a porphyritic texture composed of phenocryst (65%) of plagioclase, amphibole and biotite with a general size between 0.2 mm to 1 cm, immersed in a light grey to green groundmass due to alteration.

Microscopically, they are porphyritic rocks composed of plagioclase (60%), amphibole (20%), quartz (10%), biotite (10%) and minor (<5%) orthopyroxene, apatite and zircon phenocrysts, immersed in a fine-grained groundmass (40%) (Fig. 5f) (Table 1). Plagioclase phenocrysts are subhedral and locally altered to sericite and minor carbonates. Most of them are zoned and show simple twinning and sizes between 0.2 and 1 mm. Amphiboles show yellow to light green pleochroism (0.2-2 mm in size), while biotite shows light to dark brown pleochroism (0.5-1 mm average sized). Both of them present resorption rims. Quartz phenocrysts are embayed and with an average size of 0.6 mm.

Interpretation: Given the texture and shape of the cD lithofacies, these dacitic outcrops are interpreted as subvolcanic intrusive bodies. Their field relationship with cB (coherent basalts) and mlBr (massive lithic breccias) indicates that the cD facies can be considered as dacitic domes (Cas and Wright, 1988).

4.1.4. cR (coherent rhyolites)

In the VVF area, the coherent rhyolites (cR) usually conform semicircular bodies that are mainly intruding the cB lithofacies (coherent basalts) and locally folding them (Figs. 3, 5a). Particularly, in the Cajón de Los Nevados area, the cR lithofacies also appears as subhorizontal levels below the cB rocks and laterally associated with the cR semicircular bodies and the brecciated rhyolite lithofacies (BrR).

In general, the cR outcrops are white to orange in color due to meteoric alteration, while fresh samples have a dominant white color. They are commonly blocky and rough with a porphyritic texture, composed of medium-grained alkali feldspar, plagioclase and quartz phenocrysts in a fine-grained groundmass.

In thin section, the cR is mainly composed of alkali-feldspar (0-65%, in some cases anorthoclase), plagioclase (10-35%) and quartz (15%) and accessory amounts of biotite, apatite and zircon. Anorthoclase phenocrysts are fresh showing typical cross-hatched twinning, while, in general, alkali-feldspars are subhedral to anhedral crystals with a maximum length of 3 mm.

Quartz phenocrysts showed embayed borders and typical flash extinction. Plagioclase presents polysynthetic twinning and are less than 1 mm in length. The groundmass (70-60%) shows a fine-grained texture composed of alkali feldspar, quartz and opaque minerals and is partially altered to clays. Locally it is devitrified showing spherulitic texture.

Interpretation: The cR lithofacies are mainly considered as rhyolitic domes (Cas and Wright, 1988) due to its medium-grained to porphyritic texture, its emplacement, and the intrusive relationship with the surrounding rocks, specially affecting the cB levels. Besides, when the cR lithofacies outcrops as lava flows laterally associated with the cR domes, they are interpreted as rhyolitic coulees (Fink and Anderson, 2000).

4.1.5 BrR (brecciated rhyolite)

The brecciated rhyolite (BrR) lithofacies are laterally associated with the cR (coherent rhyolite) outcrops, partially covering them with a non-erosive contact, and mainly outcrops in the Cajón de Los Nevados area (Fig. 3).

It is characterized as a matrix-supported monomictic deposit with a brecciated texture (Fig. 5b). The BrR is composed of lithic fragments of porphyritic rhyolitic rocks in an aphanitic groundmass. The rhyolitic fragments are composed of plagioclase phenocrysts (25%) in an aphanitic groundmass (85%) and are 2 to 8 cm in length, although they can be up to 20 cm in length. Some of them also show vesicular texture.

Interpretation: Considering the above mentioned characteristics, the BrR lithofacies are effusive autoclastic deposits and represents the exposed surface of the rhyolitic lavas (coulees) and domes of the cR lithofacies and so, it is interpreted as the product of autobrecciation during the domes growth and lavas flow (McPhie et al., 1993).

4.1.6 cBd (coherent basaltic dyke)

The coherent basaltic dyke (cBd) lithofacies comprises subvertical intrusive dikes that mainly affected the cB levels, with a sharp boundary with the surrounding rocks. The cBd lithofacies outcrops in both the Cajón de Los Nevados and the Arroyo La Crianza areas. They show variable orientations between NE-SW and ENE-WSW, have 8 to 10 m thick and 80 to 150 m long and, show well-developed columnar jointing (Fig. 4h). The cBd rocks are porphyritic basaltic rocks with plagioclase and mafic phenocrysts (25%) in a dark grey aphanitic groundmass (75%).

Under the microscope, the cBd lithofacies is characterized by a porphyritic texture composed of fresh plagioclase and olivine phenocrysts (20%) in an intersertal groundmass (80%). Olivine phenocrysts (65%) are 0.5 to 2 mm in size and some of them show pyroxene reaction rims. Plagioclase phenocrysts (45%) are subhedral crystals with 0.2 to 0.5 mm in length (Fig. 4i). The groundmass is composed of plagioclase microlites, clinopyroxene, orthopyroxene and opaque minerals, while the glass is partially altered to light-brown clays.

Interpretation: The cBd lithofacies is interpreted as intrusive basaltic bodies, which show almost vertical inclinations.

4.1.7 vB (basaltic vitrophyre)

Basaltic vitrophyre lithofacies appear as subhorizontal levels (~5 m thick) in the Cajón de Los Nevados area (Fig. 3). The vB outcrops show well-developed columnar jointing and comprise porphyritic fresh black rocks with conchoidal fracture and vitreous luster, composed of plagioclase phenocrysts (45%) in a vitreous groundmass (55%) (Fig. 6d). They appear in the basal part of the cB subhorizontal outcrops in the Cajón de Los Nevados valley.

Under the microscope, the vB rocks have a vitrophyric texture composed of phenocrysts (20%) of plagioclase, orthopyroxene, clinopyroxene, and opaque minerals in a vitreous groundmass (80%). Plagioclase phenocrysts (10%) show zonation and sieve texture, are 0.2 to 1 mm in length and are mainly fresh. Orthopyroxene (5%) and clinopyroxene (3%) phenocrysts are fresh, subhedral crystals and show minor opaque mineral inclusions. Glass is usually fresh although it can appear slightly altered to brownish clays. Vitreous flow structures are common in these samples.

Interpretation: The vB is interpreted as a lava flow, whose location in the basal part of the cB lithofacies allow us to interpret them as being produced by high thermal contrast between the magma and the surface, which generated the sudden cooling of these lava flows (McPhie et al., 1993).

Lithofacies	Description	Interpretation
cB *(coherent basalt)*	Porphyritic basaltic rocks composed of plagioclase phenocrysts with variable amounts of olivine, clinopyroxene and orthopyroxene phenocrysts. Groundmass varies from intergranular to intersertal. Vesicles can be present and some outcrops show columnar jointing. They appear as massive tabular bodies and have a thickness between 10 to 20 meters.	Basaltic lava flows.
cBv *(vesicular coherent basalt)*	Porphyritic basaltic rocks showing vesicular texture. Vesicles are usually empty or locally filled with zeolites.	The uppermost level within a subaerial lava pulse.
cBd *(basaltic dyke)*	Porphyritic basaltic rocks composed of phenocrysts (20%) of fresh olivines (0.5-2 mm) and plagioclase (0.2-0.5 mm) with epitaxial growth. Groundmass (80%) is intersertal.	Subvolcanic intrusions
vB *(basaltic vitrophyro)*	Vitrophyric rocks composed of subhedral plagioclase with sieve texture, orthopyroxene with inclusions of opaque minerals, clinopyroxene and opaque minerals phenocrysts in	Basal part of cB lavas produced by sudden cooling due to high

	a vitreous groundmass (80%). Glass is almost fresh, partially altered to clays with flow structures.	thermal contrast (McPhie et al., 1993).
cA *(coherent andesite)*	Porphyritic lavas with 70% plagioclase (0.3-6 mm), 13% amphibole with brownish pleochroism and reabsorption rims, 12% orthopyroxene and 5% clinopyroxene phenocrysts immersed in an intergranular to hyalopilitic groundmass (65%).	Andesitic lava flows.
cD *(coherent dacite)*	Porphyritic rocks composed of 60% of phenocrysts of subhedral zoned plagioclase (0.2-1 mm), amphibole with yellow-green pleochroism, biotite with brownish pleochroism (0.5-1 mm), orthopyroxene, quartz and minor apatite and zircon. Fine-grained groundmass (40%) composed of feldspar, quartz and minor opaque minerals.	Dacitic domes (Cas and Wright, 1988).
cR *(coherent rhyolite)*	Porphyritic rocks with 30% phenocrysts of anorthoclase (0.5-3 mm) with polysynthetic and cross-hatched tartan pattern of twinning, plagioclase and quartz with rounded edges. Groundmass is fine-grained. The cR intrusives appears affecting the cB lavas from the middle levels. cR coulees are laterally related to cB and BrR rocks.	Subvolcanic intrusions and rhyolitic coulees (Fink and Anderson, 2000).
BrR *(brecciated rhyolite)*	Matrix-supported monomictic deposit with a brecciated texture, composed of lithic fragments of porphyritic rhyolitic rocks. Laterally and vertically associated with cR coulees and domes.	BrR are the product of autobrecciation during the flow and growth of cR coulees and domes (McPhie et al., 1993).
mLT *(massive lapilli tuff)*	Clast-supported, poorly sorted deposits mainly composed of pumice fragments with a low degree of deformation, biaxon to triaxon ash fragments, minor crystal fragments of plagioclase, quartz, amphibole, biotite and unidentified opaque minerals, and lithic fragments of vesicular basaltic rocks. The vitreous groundmass is highly fresh. mLT are interbedded with cB levels and xsLT deposits.	PDCs deposits, where elutriation of fine ash occurred in the fluid escape-dominated flow-boundary zone (Branney and Kokelaar, 2002); typical pumice pyroclastic flow deposits of McPhie et al., (1993).
bL *(thin-bedded lapilli)*	White to light-grey tabular deposits (60 cm thick), well-sorted and matrix-supported, composed of pumice fragments, basaltic lithic fragments and plagioclases crystal fragments in an ash-rich matrix; with subhorizontal thin-bedded stratification due to variable grain size. The bL are below the cB lithofacies and above the xsLT and mLT levels in the Arroyo La Crianza area.	PDCs deposited by progressive aggradation controlled by a traction-dominated flow-boundary zone (Branney and Kokelaar, 2002).
dsT *(diffuse-stratified tuff)*	White to grey thin levels (20 cm thick), composed of fine-grained pumice and ash fragments with grain sizes less than 0.06 mm that show diffuse subhorizontal lamination Interbedded with thin-bedded lapilli deposits (bL).	PDCs deposited when flow-boundary zone conditions are intermediate between fluid escape-dominated and traction-dominated flow-boundary zones (Branney and Kokelaar, 2002).
xsLT *(cross-stratified lapilli tuff)*	Matrix-supported vitreous lapilli tuff composed of pumice and ash fragments, crystal fragments of plagioclase, biotite, quartz and zircon and lithic fragments of porphyritic volcanic rocks. Pumice (1-4 mm) show elongated shapes while shards	Dilute PDCs from a traction-dominated flow (Branney and Kokelaar, 2002); typical pyroclastic

	(0.2-0.7 mm) are biaxon to triaxon with axiolitic-devitrified textures. Its outcrops show cross-stratified structures.	surge deposited (McPhie et al., 1993).
mscBr *(massive scoria breccia)*	Clast-supported rocks composed of angular scoria fragments with maximum sizes up to 20 cm. Vertically and laterally related to cBv and mlBr lithofacies.	Scoria flow deposits (McPhie et al., 1993).
mscAg-pm *(massive scoria agglomerate-pumice rich matrix)*	Matrix-supported deposits composed of accessory scoria fragments with angular shapes (5 to 60 cm size). The matrix is composed of pumice and vitreous fragments. The mscAg-pm is in erosive contact over the bL and grades upwards to mLT lithofacies.	Deposited by pyroclastic density currents (PDCs) involving particle segregation during rapid deposition of scoria clasts, fluid scape and elutriation (Branney and Kokelaar, 2002).
mlBr *(massive lithic breccia)*	Clast to matrix-supported composed of highly angular clasts with variable sizes between 3 and 50 cm, within a fine to coarse-grained sand volcaniclastic matrix. They sometimes show erosive and concave bases with variable thickness between 30 and 50 m.	Resedimented (syn-eruptive) volcaniclastic deposit due to the deposition of debris flows (McPhie et al., 1993).

Table 1. Lithofacies classification following McPhie et al. (1993), Branney and Kokelaar (2002).

***4.1.8 mLT** (massive lapilli tuff)*

The massive lapilli tuff facies (mLT) comprises massive outcrops that appears as subhorizontal and laterally discontinuous levels with a thickness between 10 to 15 m. The mLT are interbedded with the cB lithofacies with an erosive basal contact in the Cajón de Los Nevados and the Arroyo de La Crianza areas and with the xsLT (cross-stratified lapilli tuff) lithofacies nearby the Varvarco Campos Lake (Figs. 4c, 4d). These lithofacies are composed of lithic fragments of basaltic rocks (1-8 cm), together with pumice fragments (0.5-1 cm), and plagioclase crystaloclasts (less than 0.5 cm) within a fine-grained vitreous matrix (~65%).

Under the microscope, they are composed of unwelded vitroclasts (20-80%), such as pumice fragments and shards, lithic fragments (5-30%) and crystaloclasts (10-15%). The pumice fragments show elongated shapes with maximum sizes between 0.2 and 0.5 mm, while shards are biaxon and triaxon with 0.1 to 0.3 mm in size. Crystal fragments (10-15%) are composed of plagioclase, quartz with undulose extinction and biotite with brownish pleochroism and chlorite alteration (Fig. 5e). Clinopyroxene and zircon are also present. The lithic fragments (5-30%) correspond to basaltic porphyritic rocks with plagioclase and mafic phenocrysts in a vitreous groundmass.

Interpretation: Considering the massive texture, the variable, but mostly juvenile vitreous-rich composition of the pyroclastic fragments and the poor textural selection of these deposits, the mLT lithofacies comprises classical pyroclastic flows deposits (McPhie et al. 1993), associated with the deposition of pyroclastic density currents in a nearly fluid-escape dominant flow boundary zone where grains underwent low granular shear until they reach the flow boundary and finally rest (Branney and Kokelaar, 2002).

4.1.9 bL (thin-bedded lapilli)

The bL (thin-bedded lapilli) lithofacies is mainly recognized below the cB lithofacies and above the xsLT (cross-stratified lapilli tuff) and mLT (massive lapilli tuff) levels in the Arroyo La Crianza area (Figs. 3, 4d). They are white to light-grey deposits with a thickness of 60 cm. They are well-sorted and matrix-supported, composed of pumice fragments, basaltic lithic fragments and plagioclase crystal fragments in an ash-rich matrix. The bL outcrops are characterized by subhorizontal thin-bedded structure associated with a variable grain size.

Interpretation: The local continuity between bL, dsT and mLT levels indicates that the bL lithofacies deposits generated from diluted pyroclastic density currents (PDC), by progressive aggradation controlled by a traction-dominated flow-boundary zone with or without granular flow (Branney and Kokelaar, 2002).

4.1.10 dsT (diffuse-stratified tuffs)

The diffuse-stratified tuff (dsT) lithofacies outcrops as thin levels in the Arroyo La Crianza valley interbedded with thin-bedded lapilli deposits (bL). They are white to grey levels of 20 cm thick, composed of fine-grained pumice and ash fragments with grain sizes less than 0.06 mm that show diffuse subhorizontal lamination (Figs. 3, 4d).

Interpretation: Considering the well-sorted feature of these levels, dsT lithofacies are interpreted as deposited when flow-boundary zone conditions are intermediate between fluid escape-dominated and traction-dominated flow-boundary zones (Branney and Kokelaar, 2002). The systematic alternation between these dsT levels and the bL levels, can be interpreted as successive pyroclastic density currents with variable mechanisms of deposition.

4.1.11 xsLT (cross-stratified lapilli tuff)

The xsLT (cross-stratified lapilli tuff) mainly outcrops in the Arroyo La Crianza area and in the northeastern coast of the Varvarco Campos lake (Figs. 3, 4a), interbedded with massive lapilli tuff (mLT) deposits. The sxLT are described as white reddish well-sorted matrix-supported (pyroclasts: 40%, matrix: 60%) levels of 40 cm in thickness and showing cross-bedding structures. The xsLT lithofacies is composed of vitroclasts (70%) of pumice fragments with sizes between 0.5 and 2 cm and minor lithoclasts (30%) of porphyritic basaltic rocks with plagioclase and mafic phenocrysts and sizes, within 1 to 15 cm. The matrix is fine-grained.

Under the microscope, the xsLT lithofacies is characterized as matrix-supported vitreous lapilli tuffs composed mainly of vitreous fragments (55%) of elongated pumice and biaxon to triaxon shards fragments (Fig. 4b) that appear locally devitrified in an axiolytic texture. Pumice are 1 to 4 mm long, while shards present sizes between 0.2 to 0.7 mm. Plagioclase, biotite, quartz and zircon are described as crystal fragments (25%). Plagioclase presents twinned sections, zonation and is 0.2 to 0.6 mm long. Biotite fragments show brownish pleochroism and quartz fragments show subrounded edges and are less than 0.5 mm long. Lithic fragments (20%) are present as basaltic porphyritic rocks composed of plagioclase and pyroxene phenocrysts immersed in a light grey groundmass. They show subrounded shapes and are 0.5 mm long. The pyroclasts are immersed in pyroclastic matrix made of glass shards and interstitial vitreous cryptic material.

Interpretation: The xsLT (cross-stratified lapilli tuff) can be interpreted as dilute PDC deposits considering their cross-stratified structure and well-sorted texture, similarly to typically pyroclastic surge deposits according to McPhie et al., (1993). Thus, this lithofacies indicate deposition from traction-dominated flow boundaries (Branney and Kokelaar, 2002). Moreover, they are interbedded with massive lapilli tuff levels (mLT) so, all together, they are interpreted as a successive alternation of PDCs deposits, either dense (mLT) or dilute (xsLT).

4.1.12 ***mscBr*** *(massive scoria breccia)*

The massive scoria breccia (mscBr) lithofacies is described as a clast-supported deposit composed of cognate basaltic scoria clasts with sharp edges and maximum sizes of 20 cm within a fine-grained grey matrix, mostly altered to palagonite. Locally, they also present fragments of massive basaltic rocks up to 40 cm in size, with elongated flow structures. In the Arroyo La Crianza valley, they lie on the cBv (vesicular coherent basalts) lithofacies, while in the Cajón de Los Nevados valley they laterally grade to mlBr (massive lithic breccia) deposits and are vertically associated with cB levels.

Interpretation: Considering the field descriptions, the textural features and homogeneous composition of this lithofacies we interpreted them as scoria flow deposits (McPhie et al., 1993).

4.1.13 ***mscAg-pm*** *(massive scoria agglomerate-pumice rich matrix)*

The massive scoria agglomerates-pumice rich matrix (mscAg-pm) lithofacies outcrops mainly in the Arroyo La Crianza valley, with an erosive contact over the bL (thin-bedded lapilli) lithofacies and grades upwards to mLT (massive lapilli tuff) deposits (Fig. 4c). The mscAg-pm is described as a matrix-supported deposit mainly composed of accessory scoria fragments with angular shapes between 5 and 60 cm in size. The matrix is composed of fine-grained pumice and vitreous ash. The amount of scoria fragments decrease towards the top.

Interpretation: When considering their field distribution, grading vertically and laterally to mLT lithofacies, the mscAg-pm deposits can be interpreted as being deposited by pyroclastic density currents (PDC) involving particle segregation during rapid deposition of accessory scoria clasts, fluid scape and elutriation that allow the overpassing of pumice fragments and the transition to mLT dominated deposits (Branney and Kokelaar, 2002).

4.1.14 mlBr *(massive lithic breccia)*

The mlBr (massive lithic breccia) is described as poorly-sorted volcaniclastic deposits that outcrop mainly in the Cajón de Los Nevados area. They are distributed in discrete levels with 30 to 50 m width and erosive and concave bases (Figs. 5d, 6a). The mlBr are initially clast-supported and monomictic deposits, composed of lithic fragments of porphyritic basaltic rocks with sharp edges and sizes within 3 to 50 cm. Upwards the mlBr deposits become more polymictic and matrix-supported, and composed of sharped clasts of basalts and pyroclastic rocks. The mlBr deposits show a fine to coarse-grained sand volcaniclastic matrix.

Interpretation: Considering its highly brecciated character, the topography control of deposition associated with paleochannels, the absence of impact structures and its textural features, it is suggested that they are linked to a resedimented (syn-eruptive) volcaniclastic deposit due to the deposition of debris flows (McPhie et al., 1993).

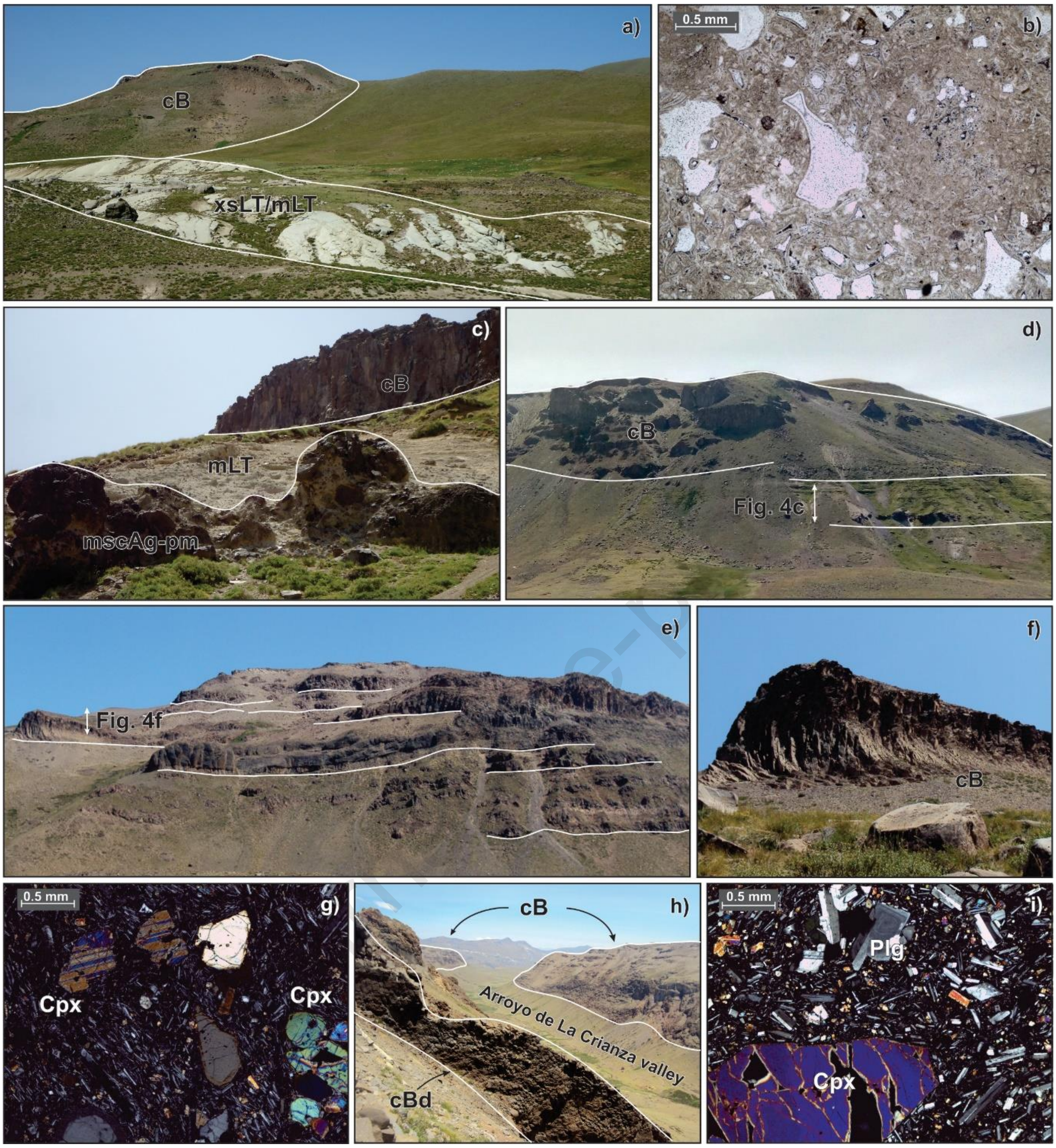

Fig. 4. (a) The cB lithofacies over xsLT and mLT levels near the Varvarco Campos Lake. (b) Microscope photograph of an xsLT sample showing biaxon and triaxon shards. (c) Basal part of profile 7a, showing mscAg-pm and mLT levels in erosive contact with cB rocks. (d) Field relationship between the basal pyroclastic lithofacies (mscAg-pm, mLT) and the subhorizontal levels of the cB in the eastern slope of the Arroyo La Crianza valley. (e) Subhorizontal cB levels in the western slope of the Arroyo La Crianza valley. (f) Detailed photograph showing cB rocks with columnar jointing. (g) Microscopic photograph of a cB sample showing clinopyroxene phenocrysts in an intergranular groundmass. (h) Subvertical basaltic dyke affecting the cB rocks. (i) Microscopic photograph of a cBd sample showing a porphyritic texture and a higher grain size than cB rocks.

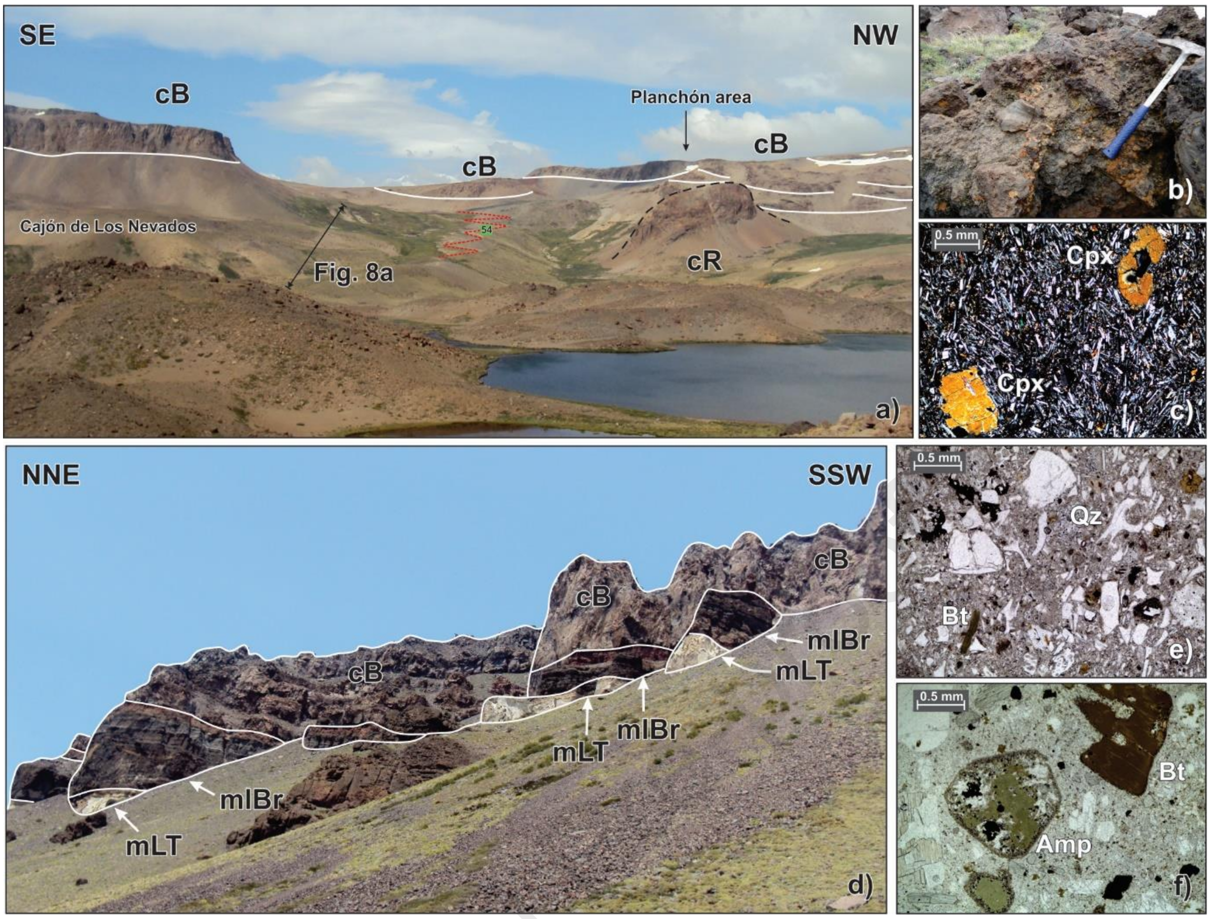

Fig. 5. (a) Western part of the Cajón de Los Nevados area representing the upper part of profile 8a (Fig. 8a), where the subhorizontal levels of the cB dominate, which are intruded by cR lithofacies (Route N°54 is shown). (b) Matrix-supported monomictic BrR deposits located in the basal levels of profile 8a. (c) Microscopic photograph of a cB sample from the Planchón area, with clinopyroxene phenocrysts. (d) The eastern extreme of the Cajón de Los Nevados area corresponds to the upper part of profile 8c. (e) Microphotograph of the mLT lithofacies, mainly composed of unwelded pumice and shard fragments, lithics and crystal fragments of biotite (Bt) and quartz (Qz). (f) Microphotograph of the cD lithofacies, showing pleochroic amphibole (Amp) and biotite (Bt) phenocrysts.

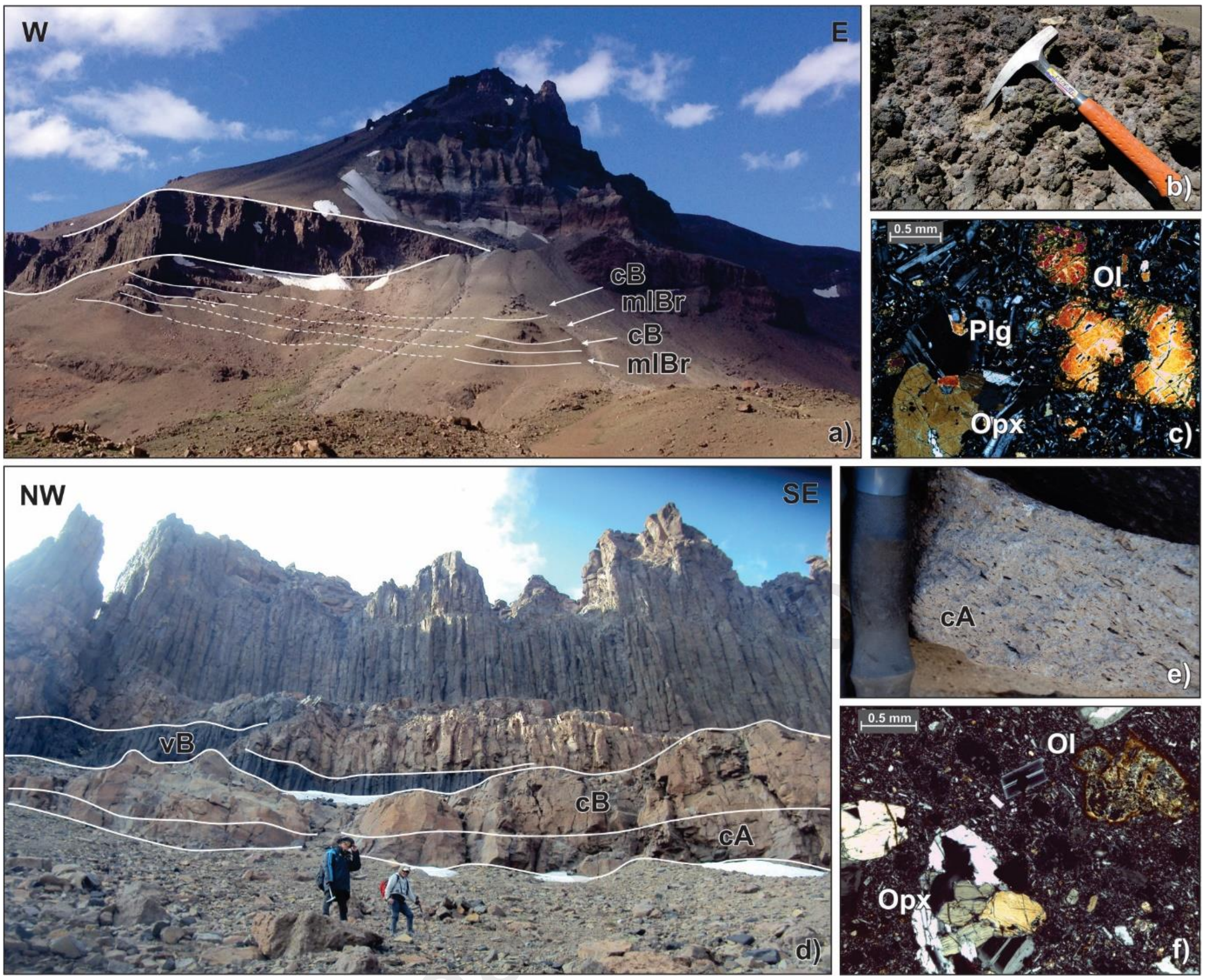

Fig. 6. (a) Northern area of the Cajón de Los Nevados valley where profile 8b has been made. (b) Monomictic massive lithic breccia (mlBr) composed of basaltic volcanic lithoclasts. (c) cB sample showing olivine, plagioclase and orthopyroxene phenocrysts in an intergranular groundmass. (d) Field photograph showing the upper section of profile 8b, where cB shows well-developed columnar jointing. (e) Andesitic sample from the cA facies, with typical porphyritic texture. (f) Basalt from the cB facies from the upper levels of profile 8b showing olivine, clinopyroxene and orthopyroxene phenocrysts.

4.2. Distribution of the Varvarco Volcanic Field lithofacies

The VVF lithofacies are distributed between two main areas: the Cajón de Los Nevados at the north and the Arroyo La Crianza valley at the south (Fig. 3) where stratigraphic profiles have been made (Figs. 7, 8). Between both areas, there is a subhorizontal basaltic plateau informally named the Planchón area.

Different structural domains influenced the emplacement of the VVF magmatism. In general, two main domains are defined: 1) N-S and NW-SE structures that show a regional continuity and involve basement rocks and, 2) NE-SW and ENE-WSW structures that are constrained within the studied area and mainly affect the VVF lithofacies.

The first domain is associated with the main structures of the Las Loicas Through (Fig. 1b), through which the VVF volcanic rocks are in tectonic contact with the intrusive bodies of the Choiyoi Group near the Varvarco Campos Lake (Figs. 1b, 2). The main NW-SE structure continues to the south and controls the emplacement of other volcanic centers such as the Domuyo and Tromen volcanic centers.

The second domain with NE-SW and ENE-WSW orientations influenced the distribution of the VVF units and is less important than the first group. Particularly, the NE-SW structures favored the emplacement of the dacitic domes (cD) in the central and northern parts of the studied area, while the ENE-WSW structures control the rhyolitic domes (cR) and the basaltic dykes (cBd) intrusions.

Considering the subhorizontal arrangement of the VVF levels, it is interpreted that the volcanic rocks in the Cajón de Los Nevados area are younger than the ones in the Arroyo La Crianza valley. The distribution of the identified lithofacies according to their temporal and spatial arrangements are described below.

4.2.1. Arroyo La Crianza valley

The basal levels of the VVF have been recognized in the Arroyo La Crianza valley. Two volcano-stratigraphic profiles allow to characterize the main lithofacies distribution in this area (Figs. 3, 4, 7). Thus, the VVF in the Arroyo La Crianza valley starts with a sequence made up of thin xsLT (cross-stratified lapilli tuff) levels interbedded with massive lapilli tuff deposits (mLT) which are associated with alternative dilute pyroclastic surge and dense pyroclastic flow deposits (Figs. 4a, 4b, 7a). This is followed by a sequence of 50 m characterized by the alternation of thin levels of diffuse-stratified tuff (dsT) and thin-bedded lapillis (bL), which is interpreted as successive pyroclastic density currents with variable mechanisms of deposition represented in discrete levels of thin thickness (Fig. 7a). To the middle part, light brown mscAg-pm (massive scoria agglomerates pumice rich-matrix) deposits are described as deposited by pyroclastic density currents (PDC) rich in accessory scoria fragments, which is followed by the mLT (massive lapilli tuff) lithofacies interpreted as dense pyroclastic density currents deposits (Figs. 4c, 4d, 7a).

The profile continues with the cB (coherent basalts) lava flows, which are dominant among the southern part of the Arroyo La Crianza area (Fig. 7a), showing well-developed columnar jointing and a subhorizontal to slight SW inclination (Figs. 4c, 4d, 4e, 4f). Lava flows are porphyritic basalts with decreasing amounts of phenocrysts, from 35% in the basal levels to 20% in the upper levels (Fig. 4g), whose mafic phases comprises olivine, clinopyroxene and orthopyroxene with vertical variable amounts along the profile (Fig. 7a). Different disequilibrium textures are recognized in these rocks, such as sieve textures in plagioclase phenocrysts and reaction rims of clinopyroxene around orthopyroxene phenocrysts. To the top of the sequence, the lava flows predominate showing important development of columnar jointing (Figs. 4e, 4f).

In the northern sector of the Arroyo La Crianza valley, represented in the profile of figure 7b, the dominant volcanic facies also correspond to the cB lavas (coherent basaltic) (Figs. 3, 4e). In this section, the VVF sequence begins with a level of scoria flow deposits (mscBr) followed by subhorizontal cB (coherent basalts) levels that comprise porphyritic basalts with a decreasing amount of phenocrysts upwards (40% to 25%) and variable type of the mafic phenocrysts phases (Fig. 7a).

Finally, the cB (coherent basalts) lithofacies are intruded by the cBd facies (coherent basaltic dyke) at the upper levels of the northern profile (Fig. 7b). They comprise two subvertical dykes: one 8 m thick and 80 m long with an ENE-WSW orientation (Fig. 4h) and the other one of 10 m thick and 150 m long with a NE-SW orientation.

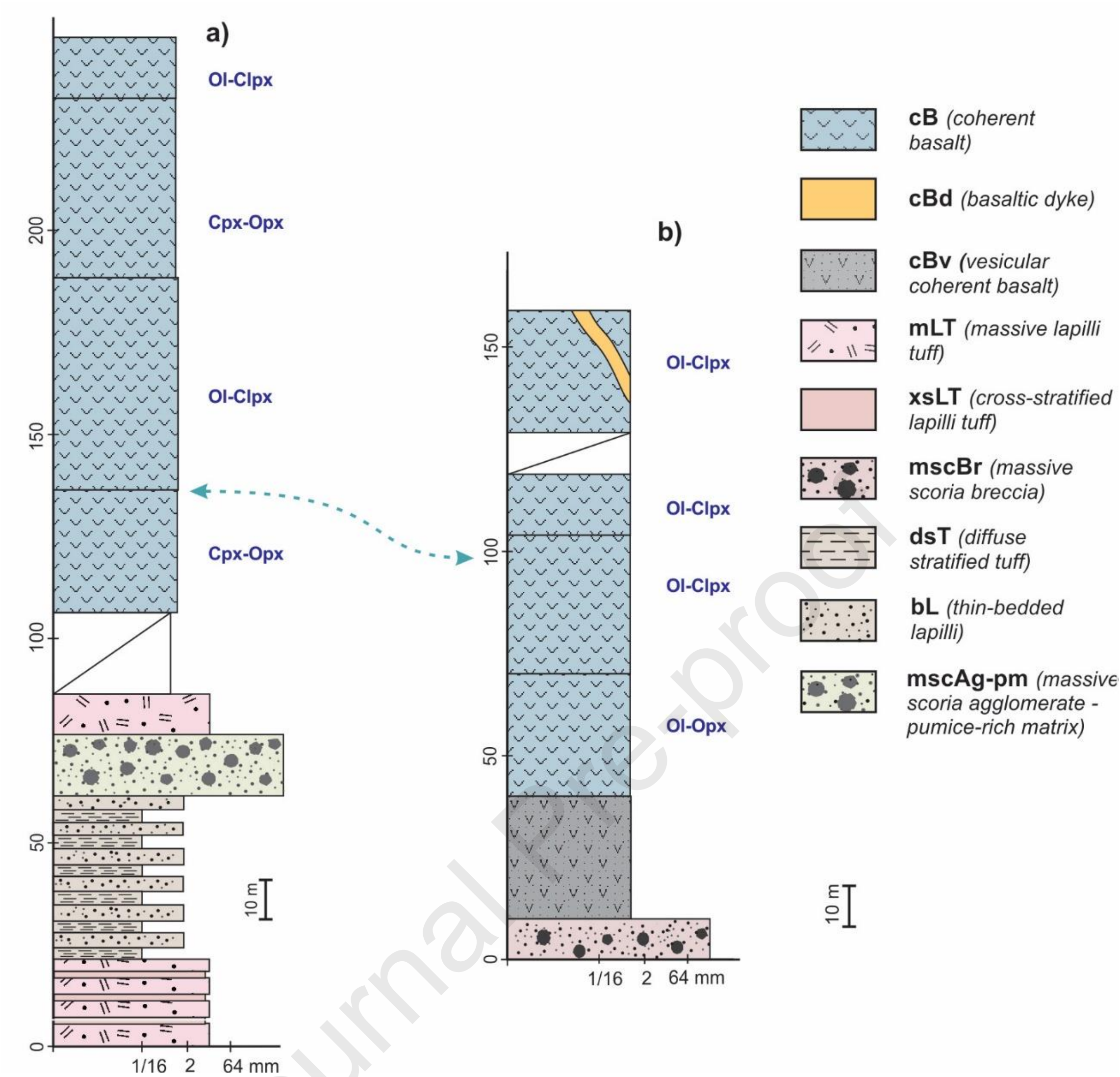

Fig. 7. (a) Stratigraphic profile at the southern extreme of the Arroyo La Crianza valley that comprises the basal levels of the VVF. (b) Stratigraphic profile in the northern area of the Arroyo La Crianza valley, which characterized the uppermost basal part of the studied sequence. The dashed light blue arrow indicates the lateral correlation between both profiles.

4.2.2. Cajón de Los Nevados area

The Cajón de Los Nevados area comprehends the northeastern sector of the Varvarco Volcanic Field (Fig. 3). Three main profiles allow to characterize both lateral and vertical variations in the upper sections of the VVF magmatism (Figs. 3, 5, 6, 8). Overall, subhorizontal levels of coherent basalts (cB) interbedded with massive lithic breccias (mlBr) are the dominant lithofacies of the Cajón de Los Nevados area (Figs. 6, 8).

The first profile is initially characterized by cR (coherent rhyolites) lava flows described as red porphyritic rocks (Fig. 8a). The cR level is interpreted as a rhyolitic coulee (Fink and Anderson, 2000), spatially related to the rhyolitic dome located to the west (Figs. 3, 5a). The cR levels are laterally in contact with BrR (brecciated rhyolites) rocks (Fig. 5b), which are interpreted as the autobrecciation of the rhyolitic coulees flow associated with the rhyolitic dome located nearby (Figs. 3, 5a). The profile continues with cB (coherent basalts) lithofacies levels that show olivine and both clinopyroxene and orthopyroxene phenocrysts as the mafic phases (Fig. 8a). Upwards, scoria flow deposits are described as massive scoria breccias (mscBr), while to the top, thick levels of subhorizontal cB (coherent basalts) comprises the informally named Planchón area (Figs. 3, 5a). They are mainly aphanitic to slightly porphyritic rocks, with dominant clinopyroxene and orthopyroxene as mafic phenocrysts, with minor olivine, contrary to the cB basal levels of this profile (Fig. 5c, 8a).

The volcanic sequence shows a lateral lithofacial variation to the north and east of the VVF area, represented by the other two profiles made within the Cajón de Los Nevados valley (Figs. 3, 8b, 8c). The profile located in the eastern extreme of the valley (Fig. 8c) is mainly composed of cB lava flows interbedded with massive lithic breccias (mlBr), the latter interpreted as resedimented (syn-eruptive) volcaniclastic deposits, such as a debris-flow (Figs. 5d, 8c). The cB lithofacies also appears in this area with a porphyritic texture composed of olivine and clinopyroxene phenocrysts as the dominant mafic phase (Figs. 5d, 8c). To the top of the profile, an mLT (massive lapilli tuff) level of low thickness but important horizontal continuity is identified, representing dense pyroclastic density currents (Figs. 5d, 5e, 8c). Within this profile, the VVF rocks are affected by a dacitic intrusive from the cD (coherent dacites) lithofacies, which have only been recognized in the Cajón de Los Nevados valley (Figs. 5f, 8c). These cD lithofacies are interpreted as elliptic domes (Cas and Wright, 1988) that affected different lithofacies among this area, such as the cB levels and the mLT deposits (Fig. 3).

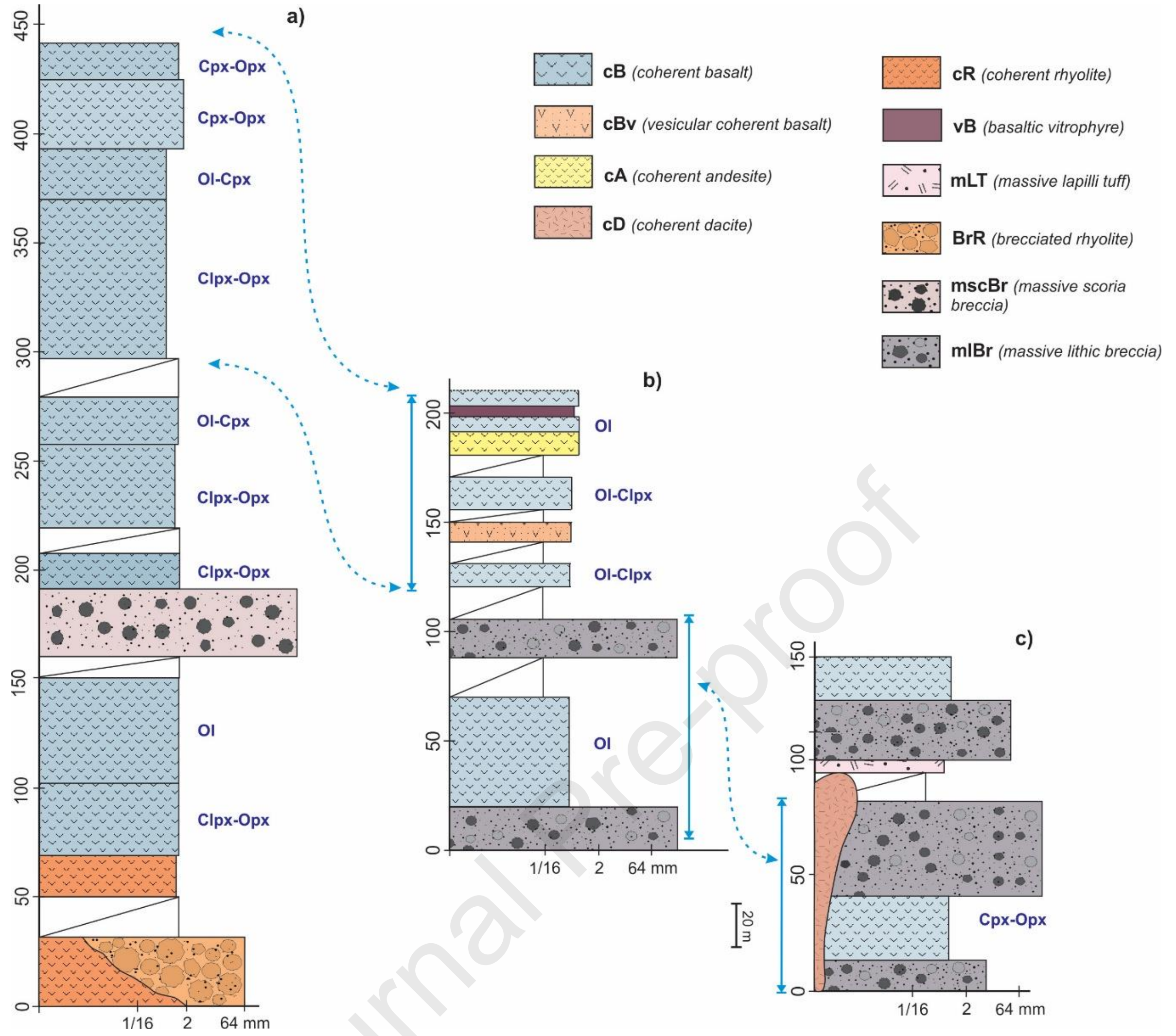

Fig. 8. Stratigraphic profiles in the eastern part of the Cajón de Los Nevados valley. The dashed light blue arrows show the lateral correlation between each other. (a) The stratigraphic profile made in the western extreme of the Cajón de Los Nevados area, which involves the cB flows of the Planchón area. (b) The profile made in the northeastern sector which is interpreted as the upper volcanic levels of the VVF. (c) The easternmost profile of the Cajón de Los Nevados represents the middle units of the VVF magmatism in this area.

The last profile of the Cajón de Los Nevados area is located in the northern side of the valley and comprises the upper levels of the studied VVF magmatism (Figs. 3, 6), represented in the profile of Figure 8b. This section is characterized by mlBr levels (massive lithic breccias), associated with debris flow deposits (Fig. 6b), interbedded with subaerial basaltic lava flows from the cB lithofacies (coherent basalts), which are correlated with the basal levels of profile 8c (Figs. 3, 6a, 8). In this case, cB levels are characterized by porphyritic volcanic rocks with mostly olivine as the dominant mafic phase in an intersertal groundmass (Fig. 6c). The middle and upper parts of the profile 8b characterized the latest volcanic episodes of the VVF magmatism. In this section, the cB lithofacies is described as porphyritic basaltic rocks with variable amounts of vesicles; olivine and clinopyroxene are dominant in the middle levels while to the top olivine prevails (Figs. 6d, 8b). Upwards, subaerial lava flows of andesitic composition, cA (coherent andesites) are described, which are followed by the basaltic vitrophyro (vB) levels (Fig. 6d, e). These two lithofacies are only identified in the upper sections of the VVF in the Cajón de Los Nevados valley. Finally, the vB is covered by basaltic lava flows, and so, they are interpreted as the basal part of this level that went into rapid cooling due to the contact with the surface (Fig. 6d).

5. Discussion

5.1. Eruptive styles of the Varvarco Volcanic Field magmatism

The Varvarco Volcanic Field shows a significant lithofacial variation throughout its eruptive history, which comprises three volcanic stages (Fig. 9). An explosive stage characterized the onset of the VVF represented by dacitic magmatism associated with the development of explosive eruptions (Fig. 9a). Initially, dilute PDCs (pyroclastic surge events) alternated with dense PDCs (pyroclastic flows), represented by xsLT and mLT lithofacies, respectively. Afterwards, successive pyroclastic density currents (PDCs) with variable mechanisms of deposition are recognized through the bL and dST lithofacies, which constitute thin-bedded lapilli and diffuse stratified tuffs deposits.

The second stage is characterized by an effusive volcanism represented by a thick succession of the cB (coherent basaltic) subaerial lava flows, with a conspicuous basaltic composition given by a plagioclase, olivine, clinopyroxene and orthopyroxene mineral assemblage (Fig. 9b). Within this stage, minor explosive events are represented by the mscAg-pm (massive scoria agglomerate-pumice rich matrix) lithofacies that corresponds to dense PDC deposits. Considering the widespread distribution and voluminous emplacement of the basaltic lava flows (cB), this second stage of the VVF could mainly represents a fissure-related volcanism associated with a Hawaiian to Strombolian eruptive style, developed within the regionally active extensional setting.

The third stage of the VVF magmatism is exposed in the Cajón de Los Nevados area, where effusive volcanism predominates, with minor explosive and resedimented (syn-eruptive) volcaniclastic deposits that alternated throughout the profile (Fig. 9c). A significant compositional variation is recognized along the effusive coherent volcanic facies, as they include mostly basaltic, but also rhyolitic and minor andesitic compositions. On the other hand, the resedimented volcaniclastic deposits are described as massive lithic breccias (mlBr) with erosive bases and lenticular shapes, associated with debris flows (Fig. 9c). The volumetrically minor explosive volcanism is associated with the mLT (massive lapilli tuff) lithofacies, related to dense PDC deposits, and the mscBr (massive scoria breccias), which are linked to scoria flows deposits; both are particularly described in the middle sections of this magmatic stage (Fig. 9c).

The upper sections of the third stage profile mostly comprise effusive basaltic volcanism, characterized by cB lava flows associated with the basaltic vitrophyre (vB) level. Remarkably, within this stage, the effusive volcanism includes a more differentiated composition towards the top of the section, whereas cB flows are interbedded with a thin andesitic lava flow (cA), and intruded by cD and cR lithofacies (Fig. 9c). These dacitic and rhyolitic intrusives also affects the uppermost basaltic levels of the second volcanic stage from the VVF, as well as minor dykes of basaltic composition (cBd lithofacies) (Fig. 9a). Dacitic and rhyolitic intrusions comprises rhyolitic coulees and domes, which are associated upwards and laterally with the brecciated rhyolites lithofacies (BrR), consequence of the rapid cooling and autobrecciation of the rhyolitic lavas and domes.

5.2. *Magmatic evolution of Varvarco Volcanic Field*

During Plio-Pleistocene times, the dominant tectonic regime changed due to variations in the subduction angle of the Nazca plate (Ramos et al. 2014; Ramos and Folguera, 2005). After a shallow subduction stage, the Nazca plate subduction angle increased causing the development of an extensional regime. During this context, the Varvarco Volcanic Field evolved simultaneously with other calderas and volcanic fields in the area (Folguera et al., 2006).

As described, initially, the VVF is characterized by a dacitic explosive volcanic stage represented by alternated dense and more dilute PDCs deposits, widely spread over the studied area (Fig. 9a). Afterwards, effusive volcanism dominates, represented by the coherent basaltic lava flows. The basaltic nature of these rocks would indicate a rapid ascend through the crust without much time to differentiate in magmatic chambers. This magmatic stage would be linked to the extensional reactivation of previous regional structures in the area; in this way, the effusive stage of the VVF, which is mainly characterized by basaltic effusive volcanism, could be associated with the regionally NO-SE main normal fault that defines the western side of the Las Loicas Trough.

Towards the last volcanic pulse of the VVF, effusive volcanism also dominates. However, while the cB lithofacies predominates, they appear interbedded with more evolved rocks corresponding to andesitic to rhyolitic lavas and intrusives. Moreover, explosive activity is also registered in the volumetrically minor dacitic PDCs deposits (mLT lithofacies) and the scoria flows deposits (mscBr) (Fig. 9c). In this sense, the lithological association of mafic effusive volcanism interbedded with more differentiate effusive and explosive magmatism, could indicate that the previous fissure-related effusive magmatic stage, turned into a more evolved effusive and explosive stage where magmatism is associated with discrete volcanic centers (Fig. 9c). The latest magmatic pulses are mostly associated with the intrusive magmatism represented by rhyolitic and dacitic domes and minor basaltic dykes, which intruded the coherent lavas facies and some of the pyroclastic deposits of the VVF. Overall, this third stage is linked to a more stabilized volcanic stage associated with the final establishment of a stratovolcano-type magmatism.

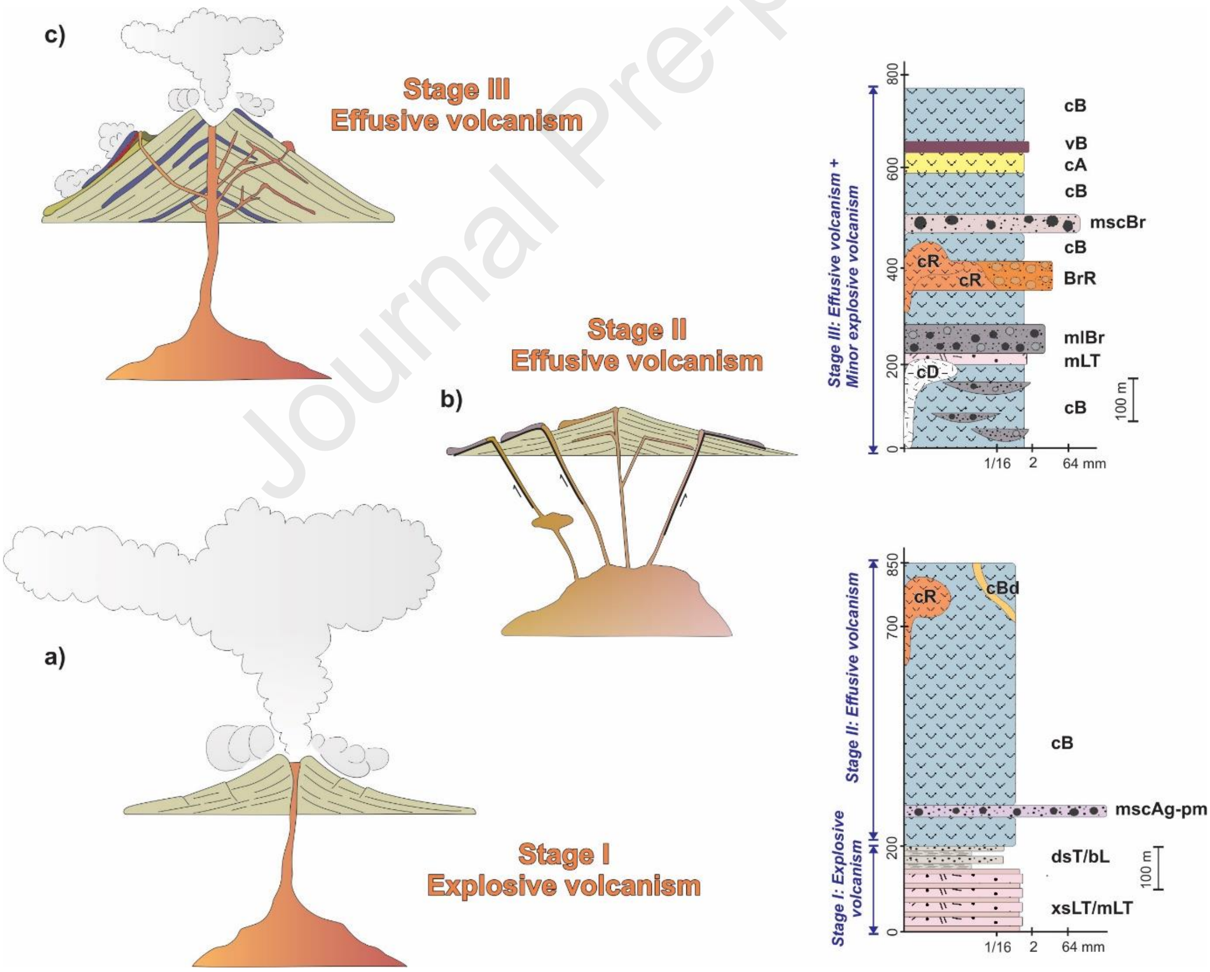

Fig. 9. Schematic model describing the emplacement of Varvarco Volcanic Field and its different eruptive stages. (a) Stage I Explosive Volcanism represented mostly by dacitic PDCs deposits. (b) Stage II Effusive Volcanism dominated by basaltic lava flows. (c) Stage III Effusive Volcanism, dominated

by basaltic and minor andesitic lavas and rhyolitic lavas flows, with minor explosive and volcaniclastic deposits, affected by dacitic and rhyolitic intrusives.

6. Conclusions

The Varvarco Volcanic Field is mainly characterized by voluminous subhorizontal basaltic lava flows and subordinate pyroclastic deposits.

The lithofacial evolution of the Varvarco Volcanic Field initiates with an explosive eruptive style. This stage is mainly represented by PDCs deposits that alternated from dense (pyroclastic flows) to more diluted (pyroclastic surges) episodes. Then, volcanism evolved into an effusive stage characterized by voluminous basaltic lava flows. This stage is interpreted as Hawaiian to Strombolian fissure-related volcanism developed within the regionally extensional regime. Finally, the last volcanic stage mainly corresponded to an effusive volcanism, with minor explosive and resedimented volcaniclastic deposits. Effusive volcanism in this stage comprises mostly basaltic lava flows, with subordinate andesitic and rhyolitic lavas, while explosive facies corresponds to PDCs and scoria flows; interbedded with debris flow deposits. The latest pulses within this stage comprise dacitic to rhyolitic intrusive bodies and minor mafic dykes. Overall, the evolution of this third stage, from mafic effusive volcanism to a more differentiated effusive and explosive one, and resedimented syn-eruptive activity, would indicate the establishment of a stratovolcano-type activity.

The magmatic development and evolution of the VVF initiates in the Early Pleistocene times, when the Nazca plate was subducting with a progressively higher angle of subduction, after the shallow subduction regime of the Middle to Late Miocene times. In consequence, this tectonic setting provoked the retraction of arc-like magmatism from east to west and an extensional regime that regionally controlled the Las Loicas Trough emplacement. The VVF magmatism show an elliptical distribution, elongated parallel to the main regional NW-SE structures. Within this context, the most conspicuous feature of the VVF is the development of the widespread and voluminous basaltic fissure-related volcanic stage.

Acknowledgements

We specially acknowledge the suggestions of both anonymous reviewers that contributed to improve the quality of the manuscript. We also acknowledge the financial support from Agencia Nacional de Promoción Científica y Tecnológica (grant PICT 2019-00974) and the University of Buenos Aires (grant UBACYT 20020190100234BA) and PIP CONICET (grant 11220200102730CO).

References

Astort, A., Colavitto, B., Sagripanti, L., García, H., Echaurren, A., Soler, S. and Folguera, A., 2019. Crustal and mantle structure beneath the southern Payenia Volcanic Province using gravity and magnetic data. Tectonics, 38 (1), 144-158.

Branney, M., Kokelaar, B., 2002. Pyroclastic Density Currents and the Sedimentation of Ignimbrites. Geological Society of London, 27, 143 pp.

Cas, R. A. F., Wright, J. V., 1988. Volcanic Successions Modern and Ancient Chapman and Hall, London, XVI, 528. https://doi.org/10.1007/978-94-009-3167-1

Cembrano, J., Lara, L., 2009. The link between volcanism and tectonics in the southern volcanic zone of the Chilean Andes: a review. Tectonophysics, 471(1-2), 96-113.

Dungan, M. A., Wulff, A., Thompson, R. E. N., 2001. Eruptive stratigraphy of the Tatara–San Pedro complex, 36°S, Southern Volcanic Zone, Chilean Andes: reconstruction method and implications for magma evolution at long-lived arc volcanic centers. Journal of Petrology, 42 (3), 555-626.

Espanon, V. R., Chivas, A. R., Turner, S. P., Kinsley, L. P., Dosseto, A., 2016. Localized magmatic constraints on continental back-arc volcanism in southern Mendoza, Argentina: the Santa Maria Volcano. Bulletin of Volcanology, 78(11), 1-13.

Fink, J. H., Anderson, S. W., 2000. Lava domes and coulees. In: Sigurdsson, H., Houghton, B., McNutt, S. R., Rymer, H., Stix, J. (Eds.), Encyclopedia of Volcanoes. Academic Press, 307–319.

Folguera, A., Zapata, T., Ramos, V. A., 2006. Late Cenozoic extension and the evolution of the Neuquén Andes. Special Papers: Geological Society of America, 407, 267.

Folguera, A., Bottesi, G., Zapata, T., Ramos, V. A., 2008. Crustal collapse in the Andean backarc since 2 Ma: Tromen volcanic plateau, Southern Central Andes (36 40′–37 30′ S). Tectonophysics, 459(1-4), 140-160.

Folguera, A., Naranjo, J. A., Orihashi, Y., Sumino, H., Nagao, K., Polanco, E., Ramos, V. A., 2009. Retroarc volcanism in the northern San Rafael Block (34–35 30′ S), southern Central Andes: Occurrence, age, and tectonic setting. Journal of Volcanology and geothermal Research, 186(3-4), 169-185.

Frey, F. A., Gerlach, D. C., Hickey, R. L., Lopez-Escobar, L., Munizaga-Villavicencio, F., 1984. Petrogenesis of the Laguna del Maule volcanic complex, Chile (36°S). Contributions to Mineralogy and Petrology, 88(1), 133-149.

Fuentes, F., Ramos, V. A., 2008. Geología de la región del cerro Guanaquero, río Diamante, Mendoza, Revista de la Asociación Geológica Argentina, 63(1), 84-96.

Galetto, A., García, V., Caselli, A., 2018. Structural controls of the Domuyo geothermal field, Southern Andes (36 38′ S), Argentina. Journal of Structural Geology, 114, 76-94.

Germa, A., Quidelleur, X., Gillot, P. Y., Tchilinguirian, P., 2010. Volcanic evolution of the back-arc Pleistocene Payún Matrú volcanic field (Argentina). Journal of South American Earth Science, 29(3), 717-730.

Gudnason, J., Holm, P. M., Søager, N., Llambías, E. J., 2012. Geochronology of the late Pliocene to recent volcanic activity in the Payenia back-arc volcanic province, Mendoza Argentina: Journal of South American Earth Sciences, 37, 191-201.

Hildreth, W., Moorbath, S., 1988. Crustal contributions to arc magmatism in the Andes of central Chile. Contributions to Mineralogy and Petrology, 98, 455-489.

Hildreth, W., Grunder, A., Drake, R., 1984. The Loma Seca Tuff and the Calabozos Caldera: A major ash-flow and caldera complex in the southern Andes of Central Chile. Geological Society American Bulletin, 9S, 4SS4.

Hildreth, W., Fierstein, J., Godoy, E., Drake, R., Singer, B., 1999. The Puelche volcanic field: extensive Pleistocene rhyolite lava flows in the Andes of Central Chile. Revista Geológica de Chile, 26, 275-309.

Hildreth, W., Godoy, E., Fierstein, J., Singer, B., 2010. Laguna del Maule Volcanic Field: Eruptive History of a Quaternary basalt-to-rhyolite distributed volcanic field on the Andean rangecrest in central Chile. Servicio Nacional de Geología y Minería, 63, 146 pp.

Hickey, R. L., Gerlach, D. C., Frey, F. A., 1984. Geochemical variations in volcanic rocks from central south Chile (33-42°S). Andean magmatism: chemical and isotopic constraints, 72-95.

Hickey-Vargas, R., Holbik, S., Tormey, D., Frey, F. A., Roa, H. M., 2016. Basaltic rocks from the Andean Southern Volcanic Zone: Insights from the comparison of along-strike and small-scale geochemical variations and their sources. Lithos, 258, 115-132.

Holm, P. M., Søager, N., Alfastsen, M., Bertotto, G. W., 2016. Subduction zone mantle enrichment by fluids and Zr–Hf-depleted crustal melts as indicated by backarc basalts of the Southern Volcanic Zone, Argentina. Lithos, 262, 135-152.

Horton, B. K., Fuentes, F., Boll, A., Starck, D., Ramirez, S. G., Stockli, D. F., 2016. Andean stratigraphic record of the transition from backarc extension to orogenic shortening: A case study from the northern Neuquén Basin, Argentina. Journal of South American Earth Sciences, 71, 17-40.

Iannelli, S.B., Medina Gallo, N., Traun, M., Astort, A., Hurley, M., Litvak, V.D., Søager, N., Folguera, A., 2022. El volcanismo plio-cuaternario de la caldera Varvarco en los Andes Centrales del Sur (36°30'S). 21° Congreso Geológico Argentino ST8, 401-402.

Iannelli, S. B., Litvak, V. D, Traun, M., Folguera, A., 2023. Evolución petrotectónica del volcanismo plio-pleistoceno del Campo Volcánico Varvarco, provincia de Neuquén (36°20'S). 14° Congreso de Mineralogía, Petrología Ígnea y Metamórfica, y Metalogénesis. Universidad Nacional del Sur.

Jacques, G., Hoernle, K., Gill, J. B., Hauff, F., Wehrmann, H., Garbe-Schönber, D., van den Bogaard, P., Bindeman, I., Lara, L. E., 2013. Across-arc geochemical variations in the Southern Volcanic Zone, 753 Chile (34.5–38°S): constraints on mantle wedge and source input compositions. Geochimica et Cosmochimica Acta, 123, 218-243. doi.org/10.1016/j.gca.2013.05.0161256.

Jacques, G., Hoernle, K., Gill, J., Wehrmann, H., Bindeman, I., Lara, L. E., 2014. Geochemical variations in the Central Southern Volcanic Zone, Chile (38–43 S): the role of fluids in generating arc magmas. Chemical Geology, 371, 27-45.

Kay, S. M., Burns, M., Copeland, P., 2006. Upper Cretaceous to Holocene magmatism and evidence for transient Miocene shallowing of the Andean subduction zone under the northern Neuquén Basin. In: Kay, S. M., Ramos, V. A. (Eds.), Evolution of an Andean margin: a tectonic and magmatic view from the Andes to the Neuquén Basin (35-39°S). Geological Society of America Special Papers, 407, 19-60.

Kleiman, L. E., Japas, M. S., 2009. The Choiyoi volcanic province at 34 S–36 S (San Rafael, Mendoza, Argentina): Implications for the Late Palaeozoic evolution of the southwestern margin of Gondwana. Tectonophysics, 473(3-4), 283-299.

Litvak, V. D., Spagnuolo, M. G., Folguera, A., Poma, S., Jones, R. E., Ramos, V. A., 2015. Late Cenozoic calc-alkaline volcanism over the Payenia shallow subduction zone, South-Central Andean back-arc (34° 30′-37° S), Argentina. Journal of South American Earth Sciences, 64, 365-380.

López-Escobar, L., Cembrano, J., Moreno, H., 1995. Geochemistry and tectonics of the Chilean Southern Andes basaltic Quaternary volcanism (37-46°S). Andean Geology, 22 (2), 219-234.

McPhie, J., Doyle, M., Allen, R., 1993. Volcanic Textures: A Guide to the Interpretation of Textures in Volcanic Rocks. University of Tasmania Centre for Ore Deposit and Exploration Studies, Hobart, p. 198.

Muñoz Bravo, J., Stern, C. R., Bermúdez, A., Delpino, D., Dobbs, M. F., Frey, F. A., 1989. El volcanismo Plio-Cuaternario a través de los 34-39°S de los Andes: Revista de la Asociación Geológica Argentina, 44, 270-286.

Narciso, V., Santamaría, G., Zanettini, J. C. M., 2004. Hoja Geológica 3769-I, Barrancas. Provincias de Mendoza y Neuquén. Instituto de Geología y Recursos Minerales, Servicio Geológico Minero Argentino, 253, 60pp.

Pallares, C., Quidelleur, X., Gillot, P. Y., Kluska, J. M., Tchilinguirian, P., Sarda, P., 2016. The temporal evolution of back-arc magmas from the Auca Mahuida shield volcano (Payenia Volcanic Province, Argentina). Journal of Volcanology and Geothermal Research, 323, 19-37.

Pallares, C., Quidelleur, X., Debreil, J. A., Antoine, C., Sarda, P., Tchilinguirian, P., Gillot, P. Y., 2019. Quaternary evolution of the El Tromen volcanic system, Argentina, based on new K-Ar and geochemical data: insights for temporal evolution of magmatic processes between arc and back-arc settings. Journal of South American Earth Sciences, 90, 338-354.

Pesce, A., 1981. Estratigrafía de las nacientes del río Neuquén y Nahuever, Provincia del Neuquén. Congreso Geológico Argentino, 8(3), 439-455.

Pesicek, J. D., Engdahl, E. R., Thurber, C. H., DeShon, H. R., Lange, D., 2012. Mantle subducting slab structure in the region of the 2010 M 8.8 Maule earthquake (30-40°S), Chile. Geophysical Journal International, 191(1), 317-324.

Ramos, V. A., Folguera, A., 2005. Tectonic evolution of the Andes of Neuquén: constraints derived from the magmatic arc and foreland deformation. Geological Society of London, Special Publications, 252(1), 15-35.

Ramos, V. A., Kay, S. M., 2006. Overview of the tectonic evolution of the southern Central Andes of Mendoza and Neuquén (35-39°S latitude). In: Kay, S. M., Ramos, V. A. (Eds.), Evolution of an Andean margin: a tectonic and magmatic view from the Andes to the Neuquén Basin (35-39°S). Geological Society of America Special Papers, 407.

Ramos, V. A., Folguera, A., 2011. Payenia volcanic province in the Southern Andes: An appraisal of an exceptional Quaternary tectonic setting. Journal of Volcanology and Geothermal Research, 201(1-4), 53-64.

Ramos, V. A., Folguera, A., Litvak, V. D., Spagnuolo, M., 2014. Andean tectonic cycle: From crustal thickening to extension in a thin crust (34-37ºSL). Geoscience Frontiers, 5, 351-36.

Schmid, R., 1981. Descriptive nomenclature and classification of pyroclastic deposits and fragments: Recommendations of the IUGS Subcommission on the Systematics of Igneous Rocks. Geologische Rundschau, 70, 794-799.

Sellés, D., Rodríguez, A., Dungan, M. A., Naranjo, J. A., Gardeweg, M., 2004. Geochemistry of Nevado de Longaví Volcano (36,2ºS): a compositionally atypical arc volcano in the Southern Volcanic Zone of the Andes. Revista Geológica de Chile, 31(2), 293-315.

Søager, N., Holm, P. M., Llambías, E. J., 2013. Payenia volcanic province, southern Mendoza, Argentina: OIB mantle upwelling in a back-arc environment: Chemical Geology, 349-350, 36-53.

Sruoga, P., Etcheverría, M. P., Feineman, M., Rosas, M., Bukert, C., Ibañes, O. D., 2012. Complejo Caldera Diamante-Volcán Maipo (34°10´S, 69°50´O): evolución volcanológica y geoquímica e implicancias en su peligrosidad: Revista de la Asociación Geológica Argentina, 69 (4:12), 508-530.

Sruoga, P., Etcheverría, M. P., Cegarra, M. I., Mescua, J., Crosta, S., Fauqué, L. E., 2016. Hoja Geológica 3569-13 Cerro Risco Plateado. Instituto de Geología y Recursos Minerales: Servicio Geológico Minero Argentino, Buenos Aires 420, 107 pp.

Sruoga, P., Elissondo, M., Rosas, M., Fierstein, J., Singer, B., Andersen, N., 2017. Cerro Barrancas, Laguna del Maule volcanic field, Chile: eruptive stratigraphy and hazard assessment. IAVCEI Scientific Assembly, Abstract VH12B, 7, 1023, Portland.

Stern, C. R., 2004. Active Andean volcanism: its geologic and tectonic setting. Revista Geológica de Chile, 31(2), 161-206.

Stern, C. R., Skewes, M. A., 1995. Miocene to present magmatic evolution at the northern end of the Andean Southern Volcanic Zone, Central Chile. Andean Geology, 22(2), 261-272.

Tapia, F., Muñoz, M., Farías, M., Charrier, R., Astaburuaga, D. 2020. Middle Jurassic-Late Cretaceous Paleogeography of the Western Margin of the Neuquén Basin (34° 30′–36° S). Opening and closure of the Neuquén Basin in the southern Andes, 269-301.

Tormey, D. R., Hickey-Vargas, R., Frey, F. A., López-Escobar, L., 1991. Recent lavas from the Andean volcanic front (33 to 42ºS); interpretations of along-arc compositional variations. In: Harmonn, R. S., Rapela C. W. (Eds.), Andean magmatism and its tectonic setting. Geological Society of America, Special Papers, 265, 57-77.

Tormey, D. R., Frey, F. A., López-Escobar, L., 1995. Geochemistry of the active Azufre-Planchón Peteroa volcanic complex, Chile (35º15'S): evidence for multiple sources and processes in a cordilleran arc magmatic system. Journal of Petrology, 36(2), 265-298.

Tunik, M., Folguera, A., Naipauer, M., Pimentel, M., Ramos, V. A., 2010. Early uplift and orogenic deformation in the Neuquén Basin: constraints on the Andean uplift from U-Pb and Hf isotopic data of detrital zircons. Tectonophysics, 489, 258–273. https://doi.org/ 10.1016/j.tecto.2010.04.017.

Turner, S. J., Langmuir C. H., Dungan M. A., Escrig S., 2017. The importance of mantle wedge heterogeneity to subduction zone magmatism and the origin of EM1. Earth Planetary and Science Letter, 472, 216–228.

Zanettini, J. C. M., 2001. Hoja Geológica 3772-II Las Ovejas, Provincia del Neuquén. Servicio Geológico Minero Argentino, Instituto de Geología y Recursos Minerales 263, 61 pp.

Highlights

- ✓ The VVF is a Plio-Pleistocene rear-arc volcanic field of the Southern Volcanic Zone.
- ✓ Volcanic activity initiated with PDCs during an explosive stage.
- ✓ Volcanism evolved into a voluminous effusive stage represented mainly by basaltic lavas.
- ✓ Finally, effusive and minor explosive stratovolcano-type activity occurred.

Declaration of interests

☒ The authors declare that they have no known competing financial interests or personal relationships that could have appeared to influence the work reported in this paper.

☐The authors declare the following financial interests/personal relationships which may be considered as potential competing interests: